LBL-26348
Preprint

Lawrence Berkeley Laboratory
UNIVERSITY OF CALIFORNIA

Materials & Chemical Sciences Division

APR 2 1 1989
LIBRARY AND DOCUMENTS SECTION

Submitted to Physical Review B

Anomalously Small 4f-5d Oscillator Strengths and 4f-4f Electronic Raman Scattering Cross Sections for Ce^{3+} in Crystals of $LuPO_4$

G.M. Williams, N. Edelstein, L.A. Boatner, and M.M. Abraham

January 1989

TWO-WEEK LOAN COPY
This is a Library Circulating Copy which may be borrowed for two weeks.

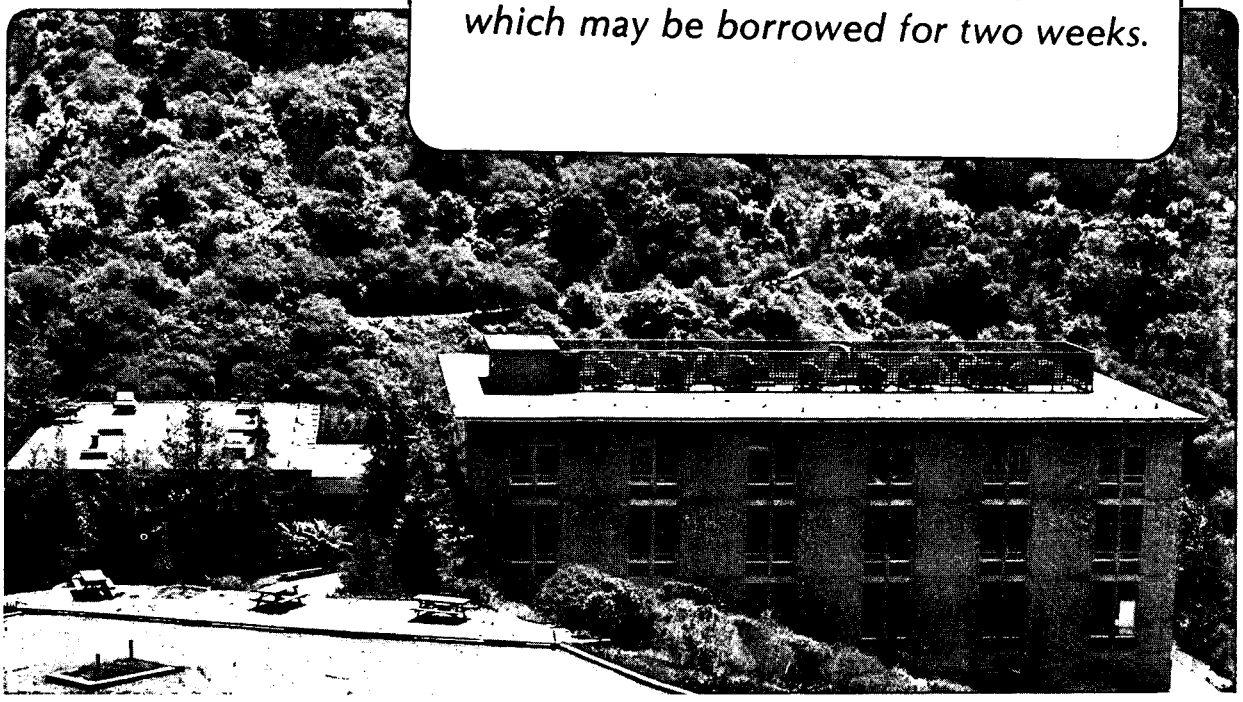

LBL-26348 c.2

Prepared for the U.S. Department of Energy under Contract Number DE-AC03-76SF00098.

DISCLAIMER

This document was prepared as an account of work sponsored by the United States Government. While this document is believed to contain correct information, neither the United States Government nor any agency thereof, nor the Regents of the University of California, nor any of their employees, makes any warranty, express or implied, or assumes any legal responsibility for the accuracy, completeness, or usefulness of any information, apparatus, product, or process disclosed, or represents that its use would not infringe privately owned rights. Reference herein to any specific commercial product, process, or service by its trade name, trademark, manufacturer, or otherwise, does not necessarily constitute or imply its endorsement, recommendation, or favoring by the United States Government or any agency thereof, or the Regents of the University of California. The views and opinions of authors expressed herein do not necessarily state or reflect those of the United States Government or any agency thereof or the Regents of the University of California.

LBL-26348

Anomalously Small 4f-5d Oscillator Strengths and 4f-4f Electronic Raman Scattering Cross Sections for Ce^{3+} in Crystals of $LuPO_4$

G.M. Williams and N. Edelstein
Department of Physics
University of California
and
Materials and Chemical Sciences Division
Lawrence Berkeley Laboratory
1 Cyclotron Road
Berkeley, California 94720 U.S.A.

L.A. Boatner and M.M. Abraham
Solid State Division
Oak Ridge National Laboratory
Oak Ridge, Tennessee 37831 U.S.A.

Abstract

The oscillator strengths for the $4f^1 \longrightarrow 5d^1$ transitions of Ce^{3+} in $LuPO_4$ were measured from absorption spectra and compared to calculated values. The measured oscillator strengths were found to be between 2.5 to 20 times smaller than the corresponding theoretical values. In addition, absolute cross sections for electronic Raman scattering between the levels of the $4f^1$ configuration of Ce^{3+} in $LuPO_4$ were measured and found to be significantly smaller than those expected from theory. Both of these discrepancies may be explained by a reduction in the radial integral, $\langle 4f|r|5d\rangle$, for Ce^{3+} in the solid state. Absorption data obtained from the literature for the $4f^1 \longrightarrow 5d^1$ transitions of Ce^{3+} in a number of host crystals were used to establish a correlation between the cerium ion-ligand distance and the reduction in the $\langle 4f|r|5d\rangle$ integral. Effects on electronic Raman scattering cross sections for rare-earth ions in crystals are discussed.

PACS numbers: 78.30.-j, 78.50.Ec, 78.20.Dj, 71.70.Ch

I. INTRODUCTION

Transparent crystals containing trivalent rare-earth ions form a unique and interesting class of optical materials, and accordingly, a great deal of effort has been directed toward establishing a quantitative description of the intensities of optical processes in these crystals. The Judd-Ofelt theory[1,2] for the intensities of the formally parity-forbidden, one-photon transitions between states of the ground $4f^N$ configuration of the trivalent rare-earth ions has proven, in general, to be quite successful–with the most notable flaw being the unexpected hypersensitivity[3–5] of one of the parameters of the theory to changes in the crystalline environment about the rare-earth ion.

The similarities between the Judd-Ofelt one-photon theory and the calculation of the intensities of two-photon transitions between states of the $4f^N$ configuration of rare-earth ions, as developed by Axe[6], have led to studies comparing the observed and calculated intensities for two-photon processes. These studies serve as a new test of the approximations common to both calculations. The two-photon experiments potentially serve as a more stringent and thus more revealing test as a result of the reduced number of parameters needed to describe the parity-allowed two-photon transitions. Comprehensive comparisons between the observed and calculated intensities have been carried out by Downer *et al.*[7–10] using two-photon absorption in crystals of Eu^{2+}:LaF_3 and Gd^{3+}:LaF_3 and by Becker *et al.*[11,12] using electronic Raman scattering in crystals of $ErPO_4$ and $TmPO_4$. The observed

discrepancies between experiment and calculation have spurred a number of papers suggesting extensions to the standard second-order theory of two-photon processes.[13–18]

Recently Judd[19] has derived a simple expression for the sum of oscillator strengths for transitions of the type $4f^N \longrightarrow 4f^{N-1}5d$. Using this expression, oscillator strength sums were computed for f$\longrightarrow$d transitions in Ce^{3+}, Tb^{3+}, and Bk^{3+} and compared to the observed values for these ions in aqueous solution[20,21]. It was found that the calculated values exceeded the observed values by factors ranging from 2 to greater than 10. This result is relevant to the intra-$4f^N$ one- and two-photon transition intensities because the expressions describing these intensities contain matrix elements of the electric dipole operator between states of the $4f^N$ and $4f^{N-1}5d$ configurations. Thus, if the measured $4f^N \longrightarrow 4f^{N-1}5d$ oscillator strengths are smaller than theoretically expected, this implies that the intensities of the intra-$4f^N$ one- and two-photon transitions also should be smaller than expected.

This idea can be readily tested by comparing the observed absolute two-photon cross sections to those calculated from theory. Many previous experiments have compared the absolute intra-$4f^N$ one-photon oscillator strengths to those computed using the Judd-Ofelt theory; but in these cases any reduction in the oscillator strengths would be absorbed in empirical parameters of the theory. To note any reduction, the values of the fitted parameters have to be compared to the values of the parameters expected from physical estimates of such quantities as the strength of the crystal field, radial overlap

integrals between configurations, and the average energies of excited configurations. The parameters of the two-photon theory are easier to estimate because they do not include the strength of the crystal field. Quantities such as the radial overlap integrals and excited configuration energies may be estimated from Hartree-Fock calculations.

In the two-photon work by Downer *et al.*[7–10] and Becker *et al.*[11,12], all intensities were calculated to within a factor that was dependent on both the radial overlap integrals and the excited configuration average energies common for all transitions. For both studies, the calculated values were compared to the experimentally observed relative intensities between different transitions–thus eliminating the necessity of the factor determining the overall scaling for the absolute cross sections.

The measurement of absolute two-photon cross sections is difficult in both electronic Raman scattering and two-photon absorption because of the problems in obtaining the efficiency of the light collection system. Chase and Payne[22] in a carefully executed experiment, however, have succeeded in measuring absolute two-photon absorption cross sections for the $^4I_{9/2} \longrightarrow {}^4G_{7/2}$ transition in Nd^{3+} doped crystals of $Y_3Al_5O_{12}$ (YAG) and $LiYF_4$ (YLF). A comparison with the calculated values showed that, for the YAG crystal, the measured cross section was as expected; but for the YLF crystal, the measured cross section was smaller than expected by approximately a factor of 10. The small value of the cross section for the YLF crystal is in accord with the reduced 4f$\longrightarrow$5d oscillator strengths noted by Judd[19].

We have recently reported the results of a comparison between the observed and calculated relative electronic Raman scattering intensities for Ce^{3+} in single crystals of $LuPO_4$.[23] Ce^{3+}, with a ground state configuration $[Xe]4f^1$, has one optically active electron. A primary motivation for the study of Ce^{3+} was the relatively low energy of the excited $5d^1$ configuration which permitted direct spectroscopic observation of these states that serve as the primary virtual intermediate states in the electronic Raman process. Thus, data has been obtained on both the electronic Raman scattering intensities and the $4f^1 \longrightarrow 5d^1$ absorption spectra. We report in this paper, a careful analysis of the absorption data and a calibration of the efficiency of the electronic Raman scattering light-collection system from which the absolute values have been obtained for both the electronic Raman scattering cross sections and the $4f^1 \longrightarrow 5d^1$ oscillator strengths. These "linked" quantities can then be compared to their respective calculated values.

II. ELECTRONIC ENERGY LEVELS AND WAVEFUNCTIONS

The wavefunctions for the states of both the $4f^1$ and $5d^1$ configuration are needed in order to compute the expected values for the $4f \longrightarrow 5d$ absorption and the $4f \longrightarrow 4f$ electronic Raman scattering cross sections. The angular parts of the wavefunctions were obtained from a parametric analysis of the observed energy levels of both the $4f^1$ ground and $5d^1$ excited configurations.[23] The energy level diagram of Ce^{3+}:$LuPO_4$ is shown in Fig. 1. The angular wavefunctions for each of the energy levels can be written as a

sum of Russell-Saunders terms:

$$|\Psi\rangle = \sum_{J,M_J} a_{J,M_J} |LSJM_J\rangle. \tag{1}$$

The radial parts of the wavefunctions are also necessary for the calculation of absolute cross sections and have been calculated numerically with a relativistic Hartree-Fock code.[24] The radial integral $\langle 4f|r|5d\rangle$ has a value of $0.441\mathring{A}$ for the Ce^{3+} free ion.

III. 4f $\longrightarrow$ 5d ABSORPTION

A. Measurement of the Oscillator Strengths

Absorption spectra of Ce^{3+} in $LuPO_4$ were obtained in the range 29,000-51,000 cm^{-1} using a Cary 17 spectrophotometer purged with dry nitrogen gas. Throughout this paper, the absorption spectra are expressed in terms of the absorbance (α), as a function of wavenumber ($k = 1/\lambda$). The absorbance is given by the usual definition,

$$\alpha(k) = -\frac{1}{l}\ln\frac{I}{I_o} , \tag{2}$$

where I_o and I are the intensities of the incident and transmitted light, respectively, and l is the crystal thickness. The oscillator strength P for a particular transition is proportional to the area under the spectral feature associated with the transition divided by the number density of absorbing ions n_o. This expression is:

$$P = \left(\frac{1}{\pi r_o}\right)\frac{1}{n_o}\int_{peak} \alpha(k)dk , \tag{3}$$

where $r_o = \frac{e^2}{m_e c^2} \approx 2.813 \times 10^{-13}$cm, and is the classical radius of the electron.

Crystals with three different doping levels of Ce^{3+} were studied. These crystals nominally had 1%, 10%, and 20% mole ratios of Ce to Lu in the starting materials used for crystal growth. In order to have a direct measure of the Ce^{3+} concentrations in the crystals, X-ray fluorescence analyses[25] were utilized on the nominally 1% and 20% crystals. The analyses showed that the actual mole percent in the crystals was reduced greatly from the starting proportions to values of 0.0604 mole% and 0.638 mole%, respectively. The number density of Lu^{3+} in $LuPO_4$[26] is 1.44×10^{22}cm^{-3} so these concentrations correspond to Ce^{3+} number densities of 8.71×10^{18}cm^{-3} and 9.19×10^{19}cm^{-3}. The relatively small values for the final Ce^{3+} concentrations are not surprising since the substitution of Ce^{3+} into Lu^{3+} sites is expected to be diminished as a result of the significantly larger ionic radius of Ce^{3+} compared to that of Lu^{3+}.[27]

The room temperature absorption spectra for crystals with the three different concentrations of Ce^{3+} are shown in Fig. 2. The peaks labelled (a),(b),(c),(d), and (f) have been previously identified[23] as $4f^1 \longrightarrow 5d^1$ transitions of Ce^{3+}. This identification is confirmed by the observation that these peaks increase with increasing Ce^{3+} concentration. For the peak labelled (a) at 31,000 cm^{-1}, the integrated absorbances for the nominally 1% and 20% crystals scale approximately as 1 to 10 in agreement with the ratio of the concentrations determined from the X-ray fluorescence analysis.

In Ce^{3+}:$LuPO_4$ it is expected that all absorption in the range 30,000 to 50,000 cm^{-1} will be solely due to the $4f^1 \longrightarrow 5d^1$ transitions of the cerium ion. Pure $LuPO_4$ is transparent[28] to approximately 70,000 cm^{-1} and transitions associated with charge transfer between the ligands and the cerium ions are expected to occur at a considerably higher energy than[29] 50,000 cm^{-1}. Reflection losses resulting from the refractive index of $LuPO_4$ are not expected to vary significantly with the excitation energy at energies so far removed from the band gap of $LuPO_4$. However, we observe in the spectra of Ce^{3+}:$LuPO_4$ absorption features which do not correlate with the cerium ion concentration. These absorption features are in the form of several well-defined peaks in the 46,000-47,500 cm^{-1} range with a broad background over the entire 30,000-50,000 cm^{-1} range. Similar features appear in the absorption spectra of pure $LuPO_4$. However, attempts to remove this background in the Ce^{3+}:$LuPO_4$ spectra by simply subtracting the $LuPO_4$ spectrum did not seem justified due to the observed variations in the background from sample to sample.

The approach utilized in carrying out the data analyses was to pick, for each concentration, a smooth background such that after subtraction the remaining spectra scaled as the known Ce^{3+} concentrations. This method seemed to work fairly well. For example, Fig. 3 shows the corrected spectrum for the nominally 20% Ce^{3+} crystal, the subtracted background, and the spectrum of a pure $LuPO_4$ crystal. The integrated absorbances for the Ce^{3+} peaks for the three different concentrations after background subtraction

are listed in Table I. The areas of the peaks at 31,000 cm^{-1} and 50,500 cm^{-1} were obtained by direct integration of the spectra. The peaks at 39,800 cm^{-1}, 42,000 cm^{-1}, and 44,500 cm^{-1} overlap significantly so that it was necessary to fit each spectrum in this region with three overlapping asymmetric gaussian functions. Although there was a certain amount of arbitrariness in these fits, the sums of the areas of the three fitted lines accurately represented the integrated absorbances for this region.

Examination of Table I indicates that, with the selected backgrounds, the absorbances scale fairly accurately. The highest error appears to occur for the peak at 50,500 cm^{-1}. This is not surprising since the largest background absorption is in this region. Table I also includes the sums of the absorbances of the Ce^{3+} peaks after background subtraction and, as an upper limit to this sum, the integrated absorbances from 30,000-50,000 cm^{-1} including the background. Oscillator strengths can be calculated easily from these values and are listed in the following section.

Spectra were taken also at 4.2 K and 77 K. The absorption spectra of a nominally 10% Ce^{3+}:$LuPO_4$ crystal taken at room temperature and at 77 K are shown in Fig. 4. The differences between the two spectra are not dramatic. There is a shift in the room temperature spectrum toward lower energies. This is probably due to absorption from thermally populated excited states which are either of vibrational or electronic origin.

B. Calculation of the Oscillator Strengths

For an ion embedded in a crystal, the oscillator strength associated with a polarized electric dipole transition between an initial state $|i\rangle$ and a final state $|f\rangle$ is given by

$$P_{fi\hat{e}} = \frac{L^2}{n}\left(\frac{4\pi\alpha_{fs}}{r_o}\right) k|\langle f|\hat{e}\cdot\vec{D}|i\rangle|^2 \tag{4}$$

where $\alpha_{fs} = \frac{e^2}{\hbar c} \approx \frac{1}{137.04}$ is the fine-structure constant, k is the wavenumber of the light absorbed in the transition, $\hat{e}$ is a unit vector describing the polarization direction of the light, $\vec{D}$ is the electric dipole operator, n is the index of refraction of the host crystal, and L is the local field correction factor. L is related to the index of refraction of the host crystal and is given by the expression,[30]

$$L = \frac{n^2+2}{3}. \tag{5}$$

$LuPO_4$ is birefringent so that the value of L is anisotropic. The values of the indices of refraction of $LuPO_4$ are assumed to be equal to the known values for the very similar crystal, YPO_4 for which $n_X = n_Y = 1.721$ and $n_Z = 1.816$ at $\lambda = 589.3$ nm.[31]

During a 4f$\longrightarrow$5d transition the vibrational state of the crystal also may change as well as the electronic state due to the difference in coupling of the lattice with the 4f electron (weak) and with the 5d electron (weak to moderate). Thus in order to accurately describe such an electronic transition, the phonon vibrational state should be included in the initial and final state descriptions. If it is assumed the Born-Oppenheimer holds (although

this may not be entirely valid for the 5d electron), the wavefunctions can be written as the product of electronic state of the rare-earth ion and the vibrational state of the crystals, i.e.

$$|f\rangle = |f_e\rangle|\chi_{f_e}^m\rangle \tag{6}$$

where $|\chi_{f_e}^m\rangle$ represents one particular vibrational mode of the crystal with the superscript m representing the occupation number of that mode. All vibrational modes may be described in a similar way.

The expression for the oscillator strength is written as

$$P_{f\hat{e}} = \frac{L^2}{n}\left(\frac{4\pi\alpha_{fs}}{r_o}\right) k|\langle f_e|\hat{e}\cdot\vec{D}|i_e\rangle|^2|\langle\chi_{f_e}^m|\chi_{i_e}^n\rangle|^2 \ , \tag{7}$$

where the vibrational part of the wavefunction has been separated out since it does not depend explicitly on the electronic coordinates of the rare-earth ion. In the absorption measurements discussed earlier, the areas under the observed broad peaks included all the transitions to a particular final electronic state. Eq. 7 can be summed over all possible final vibrational states associated with the final electronic state and, in addition, summed over all possible initial electronic states and their associated vibrational states. In the summation over initial states each term is weighted by a Boltzmann factor. With the assumption that the vibrational properties of the lattice are independent of the rare-earth ion's electronic state for all states of the 4f configuration, the summation over the vibrational quantum numbers reduces to unity.[32] The oscillator strength associated with the observed unresolved peaks can be written simply as

$$P_{f\hat{e}} = \frac{L^2}{n}\left(\frac{4\pi\alpha_{fs}}{r_o}\right) k \frac{\sum_p e^{-\beta E_{ip}} \langle f_e|\hat{e}\cdot\vec{D}|i_{ep}\rangle|^2}{\sum_p e^{-\beta E_{ip}}}, \tag{8}$$

independent of the details of the vibrational wavefunctions. This remains true when all the vibrational modes are explicitly considered.

The expression for summed oscillator strengths depends solely on the dipole matrix elements between wavefunctions describing the electronic state of the rare-earth ion. These matrix elements are most easily evaluated by expressing the operator $\hat{\mathbf{e}}\cdot\vec{D}$ as linear combinations of the spherical electric dipole operators[6], D^1_q. The values of the matrix elements for the circularly polarized dipole operators are given by

$$\begin{aligned}
\langle f_e|D^1_q|i_e\rangle = {} & \langle 5d|r|4f\rangle\langle 2||C^{(1)}||3\rangle \\
& \times \sum_{JM_J}\sum_{J'M'_J} a_{i_eJM_J} a^*_{f_eJ'M'_J} \\
& \times(-1)^{J'-M_J}\begin{pmatrix} J' & 1 & J \\ -M'_J & q & M_J \end{pmatrix} \\
& \times(-1)^{L'+S'+J+1}(2J+1)^{\frac{1}{2}}(2J'+1)^{\frac{1}{2}} \\
& \times\begin{Bmatrix} J' & 1 & J \\ L & S & L' \end{Bmatrix}\langle L'||U^1||L\rangle.
\end{aligned} \tag{9}$$

The reduced matrix element of the spherical tensor operator,$\mathbf{U}^1$, is unity for a one electron system. The value of the radial integral, $\langle 4f|r|5d\rangle$, is known from the Hartree-Fock calculations to be $0.441\mathring{A}$ for Ce^{3+}. The value of $\langle l' = 2||C^1|||l = 3\rangle$ is 1.73. No polarizers were used in the experimental measurements, so that for comparison purposes the calculated oscillator strengths are averaged over all polarizations. The light was incident along

the crystal $\hat{Y}$ axis[23] and thus the measured oscillator strengths correspond to averages of the oscillator strengths calculated for the $\hat{X}$ polarized and $\hat{Z}$ polarized electric dipole operators. Finally, all the electronic states are actually Kramers doublets so the final oscillator strengths are averaged over the oscillator strengths for the doublets of the initial states and summed over the oscillator strengths for the doublets of the final states.

C. Comparison of the Measured and Calculated Oscillator Strengths and Discussion

The results of the oscillator strength calculations are compared in Table II to the measured oscillator strengths for the nominally 20% Ce^{3+}:$LuPO_4$ crystal at both room temperature and $\sim$ 10K. There is little difference between the results for the two temperatures. The observed total 4f$\longrightarrow$5d oscillator strength is about five times smaller than the corresponding calculated value. The largest discrepancy between the calculated and measured values occurs for the transition to the highest energy level of the 5d configuration while the smallest discrepancy occurs for the transition to the lowest energy level.

The small experimental oscillator strengths are in accord with what has been observed for Ce^{3+} in aqueous solution. For that case, the 4f$\longrightarrow$ 5d oscillator strength[20] of 0.022 was approximately 2 times smaller than the value of 0.047 calculated by Judd using a partial sum rule for oscillator strengths,[19]

$$\sum_b P_{ab} = \left(\frac{2N}{7}\right) \frac{L^2}{n} \frac{\Delta E}{E_o} \langle 4f|\frac{r}{a_o}|5d\rangle^2 \ , \tag{10}$$

where a represents a state of the $4f^N$ configuration and b labels the states of the $4f^{N-1}5d$ configuration. ΔE is the energy difference (in cm^{-1}) between a and b (assumed to be constant for all b), E_o=219,475 cm^{-1}, and a_o=0.5292$\AA$. Evaluating Eq. 10 for Ce^{3+} in $LuPO_4$ yields a value for the 4f$\longrightarrow$5d oscillator strength of 0.055 which is in good agreement with the value of approximately 0.059 calculated in this paper.

A review of the literature shows that the 4f$\longrightarrow$5d oscillator strengths for Ce^{3+} in solid state systems are in general smaller than the values calculated using the Judd sum rule. A comparison of calculated and observed oscillator strengths for Ce^{3+} in various crystals is shown in Table III along with the values of the quantities used in evaluation of Eq. 10. The observed oscillator strengths were derived from various published spectra. This approach is at best very approximate. The values of the quantities that might be useful in attempts to explain the variations in 4f$\longrightarrow$5d oscillator strengths are also listed in Table III. The average Ce^{3+}-ligand distance is most obviously correlated to the oscillator strengths. The values given in the table are actually averages over the metal ion-neighboring ligand distances for the pure crystal. In general, the smaller this distance, the greater the reduction of the 4f$\longrightarrow$ 5d oscillator strength relative to the expected free ion value. This is true whether the surrounding ligands are oxygen or fluorine ions. The correlation is shown graphically in Fig. 5.

The correlation shown in Fig. 5 could reflect only the different solubili-

ties of Ce^{3+} in the various crystal hosts. In many of the earlier studies the exact concentrations of Ce^{3+} were not of crucial importance so that only starting material concentrations were reported. We have shown that the actual concentration of Ce^{3+} in a crystal can be substantially smaller than the concentration in the starting materials. An assumed value for the Ce^{3+} concentration in Eq. 3 that is too large will lead to reduced values for the oscillator strengths determined from the absorption spectra. Thus, the above correlation will follow directly if the solubility of Ce^{3+} in a crystal is related to the metal ion-ligand distance. Such a relationship might be expected for cases in which the host metal ion is smaller than the cerium ion (*i.e.* Y^{3+} and Lu^{3+}). Such a relationship does not follow as readily for the crystals CaF_2, SrF_2, BaF_2, and LaF_3, however, since in these cases the metal ion is the same size or larger than Ce^{3+} . In addition, the Ce^{3+} concentrations for $LuPO_4$ and $YAlO_3$ are known from various analyses. Thus, for a majority of the crystals, the correlation can not be explained by errors in the Ce^{3+} concentration.

A possible explanation for the correlation can be based on the neuphelauxetic effect.[33] It is generally accepted that, upon introduction of a rare earth ion into a solid state system, the rare-earth ion orbitals expand radially as a result of overlap with the ligand orbitals. This interaction of the ligand and rare-earth ion orbitals may be viewed as a first step toward covalent bonding. The effect is expected to be much greater for the 5d orbitals than for the shielded 4f orbitals. Krupke[34] has noted that a differential expansion

of the 5d orbitals relative to the 4f orbitals could lead to a substantially-reduced dipole matrix element $\langle 4f|r|5d\rangle$. This possibility becomes evident when one notes that $|4f\rangle$ and $|5d\rangle$ wavefunctions have opposite signs in some regions of space as shown in Fig. 6. The correlation of reduced 4f$\longrightarrow$5d oscillator strength with decreases in the Ce^{3+}-ligand distance can thus be seen as a consequence of the greater expansion of the 5d wavefunction as the 5d orbital-ligand orbital overlap increases.

IV. 4f $\longrightarrow$ 4f ELECTRONIC RAMAN SCATTERING

A. Measurement of the Absolute Cross Sections

The differential scattering cross section per unit solid angle per ion is defined by the relation

$$N_s = n_o l N_o \left(\frac{d\sigma}{d\Omega}\right), \tag{11}$$

where N_s is the number of photons scattered per unit time per unit solid angle, N_o is the number of photons incident on the sample per unit time, l is the sample thickness, and n_o is the number density of ions. This expression is valid in cases in which the scattering does not severely deplete the incident beam ($n_o l \frac{d\sigma}{d\Omega} \ll 1$).

If the value of N_s is known for a given transition the differential scattering cross section for that transition can be determined directly from Eq. 11. Absolute values of N_s cannot be measured directly from the scattering spectra, however, since the efficiency of the experimental light collection system

is unknown. All that can be determined directly from the spectra are the relative values of the differential scattering cross sections between different transitions.

In order to overcome this difficulty, the scattering from a crystal of $LuPO_4$ (specifically the $\hat{X}\hat{Z}$ 1,034 cm^{-1} vibrational transition) was compared to the scattering from a sample with a known scattering cross section, the 992 cm^{-1} vibrational Raman transition in benzene. The 992 cm^{-1} transition in benzene has a differential scattering cross section of 2.57×10^{-29} cm^2 per steradian of solid angle.[50] The benzene sample was contained in a quartz cuvette with the side facing the collection lens masked in order to approximate the shape and size of the $LuPO_4$ crystals. If S_c and S_b are the scattering signals measured from $LuPO_4$ and benzene, respectively, then the differential scattering cross section for the $\hat{X}\hat{Z}$ 1,034 cm^{-1} transition in $LuPO_4$ is given by

$$\left(\frac{d\sigma}{d\Omega}\right)_c = \left(\frac{S_c n_{ob} l_b}{S_b n_{oc} l_c}\right)\left(\frac{\epsilon_b}{\epsilon_c}\right)\left(\frac{d\sigma}{d\Omega}\right)_b \tag{12}$$

where all quantities are defined as in Eq. 11. The factor $\frac{\epsilon_b}{\epsilon_c}$ is a correction term to account for the differences of the indices of refraction between $LuPO_4$ and benzene. Benzene has an index of refraction of approximately 1.5[31] (and is contained in a quartz cuvette with an index of refraction of approximately 1.55[31]) while $LuPO_4$ has a refractive index of approximately 1.75. Thus reflection losses are larger and the solid angle of collection is smaller for $LuPO_4$ relative to the benzene sample. The correction factor is calculated to be approximately 1.4 for a collection lens with an f-number of 1.2. The

differential scattering cross section for the $\hat{X}\hat{Z}$ 1,034 cm^{-1} transition of $LuPO_4$ is found to be 1.28×10^{-30} cm^2 $ster^{-1}$ from the measurements of the two samples and the correction factor.

In our earlier work on electronic Raman scattering in Ce^{3+}:$LuPO_4$ all the scattering intensities were scaled relative to the $\hat{X}\hat{Z}$ 1,034 cm^{-1} Raman transition.[23] Thus, the absolute electronic Raman differential scattering cross sections can be determined from these earlier results, the value for the absolute differential scattering cross section for the $\hat{X}\hat{Z}$ 1,034 cm^{-1} Raman transition, and the actual Ce^{3+}:$LuPO_4$ concentration. The resulting differential scattering cross sections are listed in Table IV. It is estimated that these values are accurate to within a factor of 2.

B. Calculation of the Absolute Cross Sections

The differential scattering cross section for a Raman transition from an initial state $|i\rangle$ to a final state $|f\rangle$ is given by[51]

$$\frac{d\sigma}{d\Omega} = (2\pi\alpha_{fs})^2 \Lambda k k_s^3 \times \left| \sum_r \frac{\langle f|\hat{e}_s \cdot \vec{D}|r\rangle\langle r|\hat{e} \cdot \vec{D}|i\rangle}{k_{ri} - k} + \frac{[\hat{e}_s \leftrightarrow \hat{e}]}{k_{rf} + k_s} \right|^2 \tag{13}$$

where $\hat{e}$ and $\hat{e}_s$ describe the polarizations of the incident and scattered light, respectively, hck and hck_s are the energies of the incident and scattered photons, respectively, and hck_{ri} is the energy difference between the states $|r\rangle$ and $|i\rangle$. The term Λ accounts for the refractive index of the host crystal. Following Dexter,[30] an expression for Λ may be derived and is given by

$$\Lambda = \frac{n_{\hat{e}_s}}{n_{\hat{e}}} L_{\hat{e}}^2 L_{\hat{e}_s}^2 \ , \tag{14}$$

where n is the index of refraction, and L is the field correction factor given in Eq. 5.

The states $|r\rangle$ are the virtual intermediate states of the Raman process. In order for the electric dipole matrix elements to be non-zero, the states $|r\rangle$ must have opposite parity to that of the states $|i\rangle$ and $|f\rangle$. For electronic Raman scattering from rare earth crystals, the initial and final states are both associated with the rare-earth ion $4f^N$ electronic configuration so that the opposite parity states closest in energy are from the $4f^{N-1}5d$ configuration. As a first approximation, one assumes these states to be the dominant virtual intermediate states in the electronic Raman process. This assumption directly connects the electronic Raman scattering differential cross sections and the 4f$\longrightarrow$5d oscillator strengths.

In our earlier work on electronic Raman scattering in Ce^{3+}:$LuPO_4$, the relative electronic Raman scattering intensities between different transitions were computed in two ways. The first method followed Axe's standard calculation for two-photon processes in rare-earth ions.[6] This approach assumed that average values may be given to the denominators in Eq. 13 for all the states in a given configuration as in the Judd-Ofelt one photon calculation[1,2]. Closure was then performed over the states of each configuration separately. The result was an expression containing matrix elements of the spherical unit tensors U^1 and U^2, between the angular parts of the initial and final state wavefunctions and two associated radial parameters, F_1 and F_2. These

radial parameters are defined as

$$F_t(k) = (-1)^t \sum_{4f^{N-1}n'l'} \left[\frac{1}{\overline{k}_{n'l'} - k} + \frac{(-1)^t}{\overline{k}_{n'l'} + k} \right]$$

$$\times \langle 4\mathrm{f}||C^{(1)}||l'\rangle^2 \langle 4\mathrm{f}|r|n'l'\rangle^2 (2t+1)^{\frac{1}{2}} \left\{ \begin{array}{ccc} 1 & 3 & l' \\ 3 & 1 & t \end{array} \right\} \tag{15}$$

where the sum is over all excited configurations of the form $4\mathrm{f}^{N-1}n'l'$ with parity opposite that of the ground configuration. Hartree-Fock radial wavefunctions are used to explicitly evaluate F_1 and F_2 so that the absolute differential scattering cross sections can be obtained. Assuming a contribution only from the $5\mathrm{d}^1$ configuration and using a value of $\overline{k}_{5\mathrm{d}} = 40,000\mathrm{cm}^{-1}$ along with the angular terms evaluated previously[23] the differential scattering cross sections have been calculated.

The second calculation employed in the earlier work was an evaluation of the sum over intermediate states using the angular parts of the $4\mathrm{f}^1$ and $5\mathrm{d}^1$ wavefunctions obtained from crystal field fits. The absolute differential scattering cross sections are obtained by simply scaling these results by $|\langle 4\mathrm{f}|r|5\mathrm{d}\rangle|^4 |\langle 2||C^{(1)}||3\rangle|^4$.

C. Comparison Between the Measured and Calculated Cross Sections

A comparison between the observed and calculated differential scattering cross section is given in Table V. In this table the cross sections have been averaged over polarizations and summed over the crystal-field levels of each Russell-Saunders multiplet. The comparison shows that the observed dif-

ferential cross sections are smaller than both sets of calculated values. The calculation using the closure approximation, however, yields values closer to the observed values than the calculation in which the $5d^1$ wavefunctions and energies are explicitly used. This is surprising in that it has been shown[23] that the explicit calculation predicts the relative electronic Raman differential scattering cross sections much more accurately.

To rationalize these results, one has to look at the previous discussion of 4f$\longrightarrow$5d oscillator strengths. The 4f$\longrightarrow$5d oscillator strengths for Ce^{3+} in $LuPO_4$ are, on the average, 5.3 times smaller than calculated. For the lowest energy 5d level, the observed oscillator strength is 2.5 times smaller than the calculated value. We have suggested that this reduction results from a decrease in the value of the radial integral $\langle 4f|r|5d\rangle$ in the solid state relative to the free or gaseous state. It follows that the electronic Raman differential scattering cross sections should be reduced by factors on the order of $(2.5)^2 \approx 6.3$ to $(5.3)^2 \approx 30$. It can be seen from Table V that the results of the explicit calculation fall into this range.

A more detailed calculation may be performed if an assumption is made regarding the nature of the reduction in the radial integral $\langle 4f|r|5d\rangle$. The measured oscillator strengths are smaller than their respective calculated values by factors ranging from 2.5 to 19. In the above estimate we used the reduction factor for the lowest $5d^1$ level and the average reduction factor for the entire $5d^1$ configuration to calculate the expected reduction of the electronic Raman scattering cross sections. A more accurate description

would include all the reduction factors. Accordingly a calculation has been made in which each term in the summation over the $5d^1$ states in Eq. 13 is weighted by a factor given by the square root of the ratio of the measured oscillator strength to the calculated oscillator strength for that particular $5d^1$ state. The differential scattering cross sections are then given by

$$\frac{d\sigma}{d\Omega} = (2\pi\alpha_{fs})^2 \Lambda k k_s^3 \left| \sum_r \zeta_r A_{ifr} \right|^2 , \tag{16}$$

where,

$$A_{ifr} = \frac{\langle f|\hat{e}_s \cdot \vec{D}|r\rangle\langle r|\hat{e} \cdot \vec{D}|i\rangle}{k_{ri} - k} + \frac{[\hat{e}_s \leftrightarrow \hat{e}]}{k_{rf} + k_s} , \tag{17}$$

and

$$\zeta_r = \sqrt{\frac{\text{meas. osc. strength}_r}{\text{calc. osc. strength}_r}}. \tag{18}$$

This calculation is justified as long as the reduction factor associated with a given 4f→5d transition ζ_r is independent of the particular 4f state under consideration. In other words, we have assumed that the reduction in the radial overlap integral results solely from the expansion of the 5d orbitals and that the 4f orbitals retain their free ion radial distributions.

The results of the weighted calculation are compared to the measured cross sections in Tables V and VI and the earlier results of the explicit calculation without weighting. The comparison is surprising in the degree to which the weighted calculation agrees with the measured values of the differential scattering cross sections. This agreement may be somewhat fortuitous given the large uncertainty in the measurement of the cross sections (a factor of 2). Even given this error, however, the results of the calculation with

weighting are impressive. In addition, examination of Table V and Table VI shows that the the calculation with weighting offers a slight improvement over the calculation without weighting in describing the relative values of the cross sections for the different transitions.

The above discussion is based on the assumption that the states of the $5d^1$ electronic configuration serve as the primary intermediate channels in the electronic Raman scattering process. The results of the present work seem to indicate that this is the case for Ce^{3+} in $LuPO_4$. This may not, however, be the case in general. The results of several one and two-photon intensity experiments in rare-earth solids are most readily explained by the inclusion of g-orbital effects.[14,34,52,53] If all the g-orbitals are considered to be degenerate in energy, it can be shown[1] by closure that their contribution to the electronic Raman scattering process is proportional to $|\langle 4f|r^2|4f\rangle|^2$. As pointed out most recently by Chase and Payne[22] and earlier by Krupke[34], this radial integral does not vary significantly with the radial expansion of the rare-earth ion orbitals. In addition, in the solid-state the energy of the g type orbitals may be substantially reduced from the free-ion values. Thus, one can imagine situations in which these orbitals contribute significantly to the electronic Raman scattering process. In such cases, the $4f \longrightarrow 5d$ oscillator strengths could be much smaller than expected with electronic Raman cross sections not being proportionally reduced.

V. CONCLUSIONS

For Ce^{3+} in $LuPO_4$ the intensities of the two parity-allowed optical processes, 4f$\longrightarrow$5d absorption and 4f$\longrightarrow$4f electronic Raman scattering, are both smaller than expected from calculations based on free-ion estimates of the radial wavefunctions. These results can be explained in terms of a reduction of the radial integral $\langle 4f|r|5d\rangle$ in the solid state. Furthermore, a compilation of data on 4f$\longrightarrow$5d oscillator strengths for Ce^{3+} in other crystal hosts shows that a reduction in the value of this radial integral is correlated with the Ce^{3+}-ligand distance. The nearer the ligands are to the cerium ion, the greater the reduction. It is suggested that a reduction in the value of the $\langle 4f|r|5d\rangle$ does not always result in a corresponding reduction in the electronic Raman cross section, however, if contributions from intermediate states other than those associated with $4f^{N-1}5d^1$ configuration are significant.

VI. ACKNOWLEDGEMENTS

We would like to thank B. R. Judd for initially pointing out to us the discrepancies between observed and calculated f$\longrightarrow$d oscillator strengths and for supplying us with a preprint of Ref. 19. Thanks also goes to Xia Shangda and J.A. Koningstein for helpful suggestions and for critical review of the manuscript. Finally we would like to thank Robert Giauque and Linda Sindelar for performing the X-ray fluorescence analysis.

This research was supported in part by the Director, Office of Energy

Research, Office of Basic Energy Science, Chemical Sciences Division, the U.S. Department of Energy, under contract no. DE-AC03-76SF00098. Oak Ridge National Laboratory is operated by Martin Marietta Energy Systems Inc., for the U.S. Department of Energy, under contract no. DE-AC05-84OR21400.

REFERENCES

[1]B.R. Judd, Phys. Rev. **127**, 750 (1962).

[2]G.S. Ofelt, J. Chem. Phys. **37**, 511 (1962).

[3]C.K. Jørgensen and B.R. Judd, Mol. Phys. **8**, 281 (1964).

[4]S.F. Mason and R.D. Peacock, Mol. Phys. **30**, 1829 (1975).

[5]R.D. Peacock, Structure and Bonding **22**, 88 (1975).

[6]J.D. Axe, Phys. Rev. **136A**, 42 (1964).

[7]M. Dagenais, M. Downer, R. Neumann, and N. Bloembergen, Phys. Rev. Lett. **46**, 561 (1981).

[8]M.C. Downer, A. Bivas, and N. Bloembergen, Opt. Comm. **41**, 355 (1982).

[9]M.C. Downer and A. Bivas, Phys. Rev. B **28**, 3677 (1983).

[10]Michael Coffin Downer, *Two-Photon Spectroscopy of Rare Earth Ions in In Condensed Matter Environments.* PhD thesis, Harvard University, February 1983.

[11]P.C. Becker, N. Edelstein, G.M. Williams, J.J. Bucher, R.E. Russo, J.A. Koningstein, L.A. Boatner, and M.M. Abraham, Phys. Rev. B **31**, 8102 (1985).

[12]Philippe C. Becker, *Electronic Raman Scattering in Rare Earth Phosphate Crystals.* PhD thesis, University of California, Berkeley, November 1986. LBL-22634.

[13]B.R. Judd and D.R. Pooler, J. Phys. C: Solid State Phys. **15**, 591 (1982).

[14]P.C. Becker, N. Edelstein, B.R. Judd, R.C. Leavitt, and G.M.S. Lister, J. Phys. C **18**, L1063 (1985).

[15]J. Sztucki and W. Stręk, Phys. Rev. B **B34**, 3120 (1986).

[16]J. Sztucki and W. Stręk, Chem. Phys. Letters **125**, 520 (1986).

[17]J. Sztucki and W. Stręk, Chem. Phys. Letters **138**, 410 (1987).

[18]M.F. Reid and F.S. Richardson, Phys. Rev. B **B29**, 2830 (1984).

[19]B.R. Judd, Inorganic Chimica Acta **139**, 341 (1987).

[20]W.T. Carnall, *Handbook on the Physics and Chemistry of Rare Earth Ions in Solution* (North-Holland, Amsterdam, 1979).

[21]J.V. Beitz W.T. Carnall and H. Crosswhite, J. Chem. Phys. **80**, 2301 (1984).

[22]L.L. Chase and S.A Payne, Phys. Rev. B **34**, 8883 (1986).

[23]G.M. Williams, P.C. Becker, N. Edelstein, J.G. Conway, L.A. Boatner, and M.M. Abraham to be submitted to Phys. Rev. B.

[24]R.D. Cowan, *The Theory of Atomic Structure and Spectra* (University of California Press, Berkeley, 1981).

[25]R.D. Giauque, R.B. Garrett, and L.Y. Goda, Anal. Chem. **49**, 1012 (1977).

[26]W.O. Milligan, D.F. Mullica, G.W. Beall, and L.A. Boatner, Inorg. Chim. Acta **60**, 39 (1982).

[27]F.A. Cotton and G. Wilkinson, *Advanced Inorganic Chemistry*, fifth ed. (John Wiley and Sons, Inc., New York, 1988).

[28]E. Nakazawa and F. Shiga, J. of Luminescence **15**, 255 (1977).

[29] Charge transfer bands for Ce^{3+} should occur at an energies considerably higher than those observed for Yb^{3+} in the same crystal host. In Yb^{3+}:$LuPO_4$ the onset of the first charge transfer band has been observed[54] at approximately 48,500 cm^{-1}.

[30]D.L. Dexter, "Optical properties of dielectric solids," in *Solid State Physics no. 6, Advances in Research and Application*, (edited by F. Seitz and T. Turnbull), (Academic Press Inc., New York, 1958).

[31]R.C. Weast, *CRC Handbook of Physics and Chemistry, 59th Edition* (CRC Press Inc., West Palm Beach, Florida, 1978-1979).

[32]C. J. Ballhausen, *Molecular Electronic Structures of Transition Metal Complexes* (McGraw-Hill, Inc., Great Britain, 1979).

[33]R. Reisfeld and C.K. Jørgensen, *Lasers and Excited States of Rare Earths, Inorganic Chemistry Concepts vol. 1* (Springer-Verlag, Berlin, 1977).

[34]W.F. Krupke, Phys. Rev. **145**, 325 (1966).

[35]R.W.G. Wyckoff, *Crystal Structures*, Vol. 3 (John Wiley and Sons, New York, 1965).

[36]T.S. Lomheim and L.G. Deshazer, Phys. Rev. B **20**, 4343 (1979).

[37]W.J. Miniscalco, J.M. Pellegrino, and W.M. Yen, J. Appl. Phys. **49**, 6109 (1978).

[38]K. Okada, Y. Kaizu, H. Kobayashi, K. Tanaka , and F. Marumo, Mol. Phys. **54**, 1293 (1985).

[39]S. Geller and E.A. Wood, Acta Cryst. **9**, 563 (1956).

[40]M.J. Weber, B.H. Matsinger, V.L. Donlan and G.T. Stuart, J. Chem. Phys. **57**, 562 (1972).

[41]M.J. Weber, J. Appl. Phys. **44**, 3205 (1973).

[42]P. Blanchfield and G.A. Saunders, J. Phys. C: Solid State Phys. **12**, 4673 (1979).

[43]D.E. Castleberry and A. Linz, Appl. Opt. **14**, 2506 (1975).

[44]D.J. Ehrlich, P.F. Moulton, and R.M. Osgood, Jr., Opt. Lett. **4**, 184 (1979).

[45]R.W.G Wyckoff, *Crystal Structures*, Vol. 1 (John Wiley and Sons, New York, 1965).

[46]E. Loh, Phys. Rev. **154**, 270 (1967).

[47]A. Zalkin and D.H. Templeton, Acta Cryst. B **41**, 91 (1985).

[48]M.P. Wirich, Appl. Opt. **5**, 1966 (1966).

[49]D.J. Ehrlich, P.F. Moulton, and R.M. Osgood, Jr., Opt. Lett. **5**, 339 (1980).

[50]A.Yariv, *Quantum Electronics* (John Wiley and Sons, New York, 1975).

[51]R. Loudon, *The Quantum Theory of Light* (Clarendon Press, Oxford, 1983).

[52]P.J. Becker, Phys. Stat. Sol. (b) **43**, 583 (1971).

[53]M. Hasunama, K. Okada, and Y. Kato, Bull. Chem. Soc. Japan. **57**, 3036 (1974).

[54]Glen M. Williams, *Resonance Electronic Raman Scattering in Rare Earth Crystals.* PhD thesis, University of California, Berkeley, December 1988. LBL-26344.

Absorption Peak cm^{-1}	Integrated Absorbances $\times 10^{-3}$, cm^{-1}		
	x=.01	x=.10	x=.20
31,000	31.4	120.3	299.9
39,800	40.9	117.5	395.0
42,000	13.3	67.7	150.6
44,500	6.9	28.1	79.7
50,500	3.0	32.5	66.1
Sum for all peaks	95.5	366.1	991.3
Sum with Background	529.7	1,215	1,682

TABLE I. Room temperature integrated absorbances for $Ce_xLu_{1-x}PO_4$ where x represents the proportion of Ce^{3+} in the starting materials.

Peak	T=10K			T=295K		
	$P \times 10^2$		Ratio	$P \times 10^2$		Ratio
cm^{-1}	Calculated	Observed	$\frac{calc}{obs}$	Calculated	Observed	$\frac{calc}{obs}$
30,468	0.88	0.35	2.5	0.86	0.37	2.3
39,931	1.05	0.36	2.9	2.21	0.49	4.5
41,626	0.81	0.20	4.1	0.63	0.19	3.3
44,038	0.40	0.05	8.0	0.44	0.10	4.4
50,290	2.7	0.14	19	1.98	0.08	25
Total	5.8	1.1	5.3	6.12	1.23	5.0

TABLE II. Observed and calculated oscillator strengths for the nominally 20% Ce^{3+}:$LuPO_4$ crystal at temperatures of 10K and 295K.

Host Crystal	coordi-nation	M-L ($\AA$)	$\overline{\Delta E}$(cm^{-1})	lowest 5d(cm^{-1})	n	P_{calc} $\times 10^2$	P_{obs} $\times 10^2$
$LuPO_4$	8	2.309[a]	41,570	30,700	1.75[b]	5.5[c]	1.24[d]
YAG[e]	8	2.368[f]	34,200	22,040	1.9[g]	5.7	0.57[h]
aquo	9	2.575[i]	44,000	39,000	1.3[j]	4.7	2.2[k]
$YAlO_3$	9	2.62[k]	37,940	32,920	2[l]	6.9	4.0[m]
YLF	8	2.269[n]	43,690	34,270	1.5[o]	5.3	0.48[p]
CaF_2	8	2.364[q]	44,500	32,400	1.434[r]	5.1	1.7[s]
SrF_2	8	2.511[q]	45,730	33,600	1.442[r]	5.3	2.5[s]
LaF_3	9	2.52[t]	44,380	40,600	1.6[u]	5.8	2.1[v]
BaF_2	8	2.685[q]	45,940	34,200	1.475[r]	5.5	4.4[s]

[a]Ref. 26, [b]Ref. 31, [c]calculated using Eq. 11, [d]this work, [e]Only four of an expected five $5d^1$ levels were observed due to the transmission cutoff of the YAG crystal. [f]Ref. 35, [g]Ref. 36, [h]Ref. 37, [i]Ref. 38, [j]Ref. 31, [k]Ref. 39, [l]Ref. 40, [m]Ref. 41, [n]Ref. 42, [o]Ref. 43, [p]Ref. 44, [q]Ref. 45, [r]Ref. 46, [s]Ref. 31, [t]Ref. 47, [u]Ref. 48, [v]Ref. 49.

TABLE III. Comparison between calculated and observed 4f$\longrightarrow$5d oscillator strength for Ce^{3+} in various host crystals. M-L is the average metal ion-ligand distance. $\overline{\Delta E}$ is the average $5d^1$ energy. n is the refractive index used in Eq. 11.

Transition	$\frac{d\sigma}{d\Omega} \times 10^{30}$, cm^2/steradian				
Δcm^{-1}	$\hat{X}\hat{Y}$	$\hat{Z}\hat{Z}$	$\hat{X}\hat{Z}$	$\hat{Z}\hat{Y}$	all pol.
240	0.6	0	0	0	0.3
429	1.6	1.2	9.5	2.5	7.4
2,179	0.5	1.8	1.1	3.1	3.25
2,221	1.7	0	1.9	0.2	1.9
2,620	0.7	0	1.8	0.2	1.35
2,676	0.6	0	0.5	0	0.55

TABLE IV. Measured differential scattering cross sections for electronic Raman scattering in Ce^{3+}:$LuPO_4$.

Transition	$\frac{d\sigma}{d\Omega} \times 10^{30}$,cm^2/steradian			
	Observed	Calculated Judd-Ofelt	Calculated 5d Wavefunctions	Calculated Weighted 5d Wavefunctions
$^2F_{5/2} \longrightarrow {}^2F_{5/2}$	7.7	76.8	105	10.6
$^2F_{5/2} \longrightarrow {}^2F_{7/2}$	7.1	9.0	35.5	7.2

TABLE V. Observed and calculated electronic Raman differential scattering cross sections for Ce^{3+} in $LuPO_4$. The transition $^2F_{5/2} \longrightarrow {}^2F_{5/2}$ includes transitions from the ground state to the levels at 240 cm^{-1} and 429 cm^{-1}. The transition $^2F_{5/2} \longrightarrow {}^2F_{7/2}$ includes transitions from the ground state to the levels at 2,179 cm^{-1}, 2,221 cm^{-1}, 2,620 cm^{-1}, and 2,676 cm^{-1}.

Transition Δcm^{-1}	$\frac{d\sigma}{d\Omega} \times 10^{30}$,cm^2/steradian		
	Observed	Calculated 5d Wavefunctions	Calculated Weighted 5d Wavefunctions
240	0.3	31	2.8
429	7.4	74	7.8
2,179	3.25	20	2.9
2,221	1.9	5.3	1.9
2,620	1.35	6.7	1.9
2,676	0.55	3.5	0.5

TABLE VI. Observed and calculated electronic Raman differential scattering cross sections for Ce^{3+} in $LuPO_4$.

FIGURE CAPTIONS

FIG. 1. Schematical representation of energy level structure of Ce^{3+} in a crystal of $LuPO_4$. All numbers are in cm^{-1}.

FIG. 2. Room temperature absorption spectra of Ce^{3+}:$LuPO_4$ for three different concentrations of Ce^{3+}. The peaks labelled (a),(b),(c),(d), and (f) are attributed to absorption in cerium. The peak (e) is due to an impurity.

FIG. 3. (a) Room temperature absorption spectrum for the nominally 20% Ce^{3+}:$LuPO_4$ crystal with background absorption subtracted. (b) Simulated background absorption. (c) Room temperature absorption spectrum of $LuPO_4$.

FIG. 4. Room temperature and 77K absorption spectra of the nominally 10% Ce^{3+}:$LuPO_4$.

FIG. 5. Plot of the ratio of observed over calculated oscillator strength vs. the average $Metal^{3+}$-ligand distance in Å. Oxide crystals are labelled with circles while fluoride crystals are labelled with inverted triangles. The oscillator strengths were calculated using the Judd sum rule, Eq. 11.

FIG. 6. Hartree-Fock calculated radial wavefunctions for the 4f and 5d orbitals of Ce^{3+}. The functions plotted are actually $r|4f\rangle$ and $r|5d\rangle$.

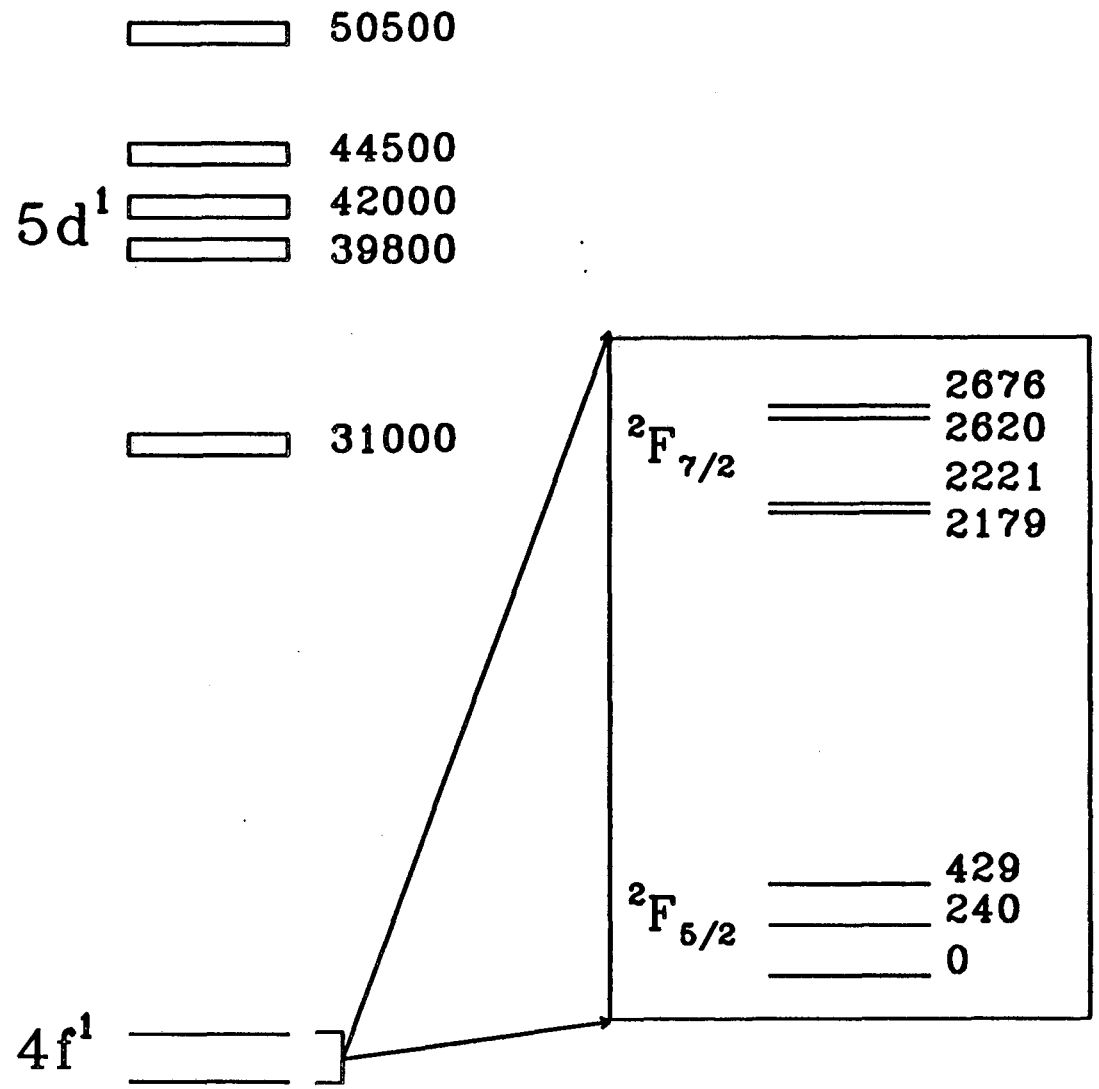
50500
44500
5d¹
42000
39800
31000
4f¹
²F 7/2
2676
2620
2221
2179
²F 5/2
429
240
0

Figure 1

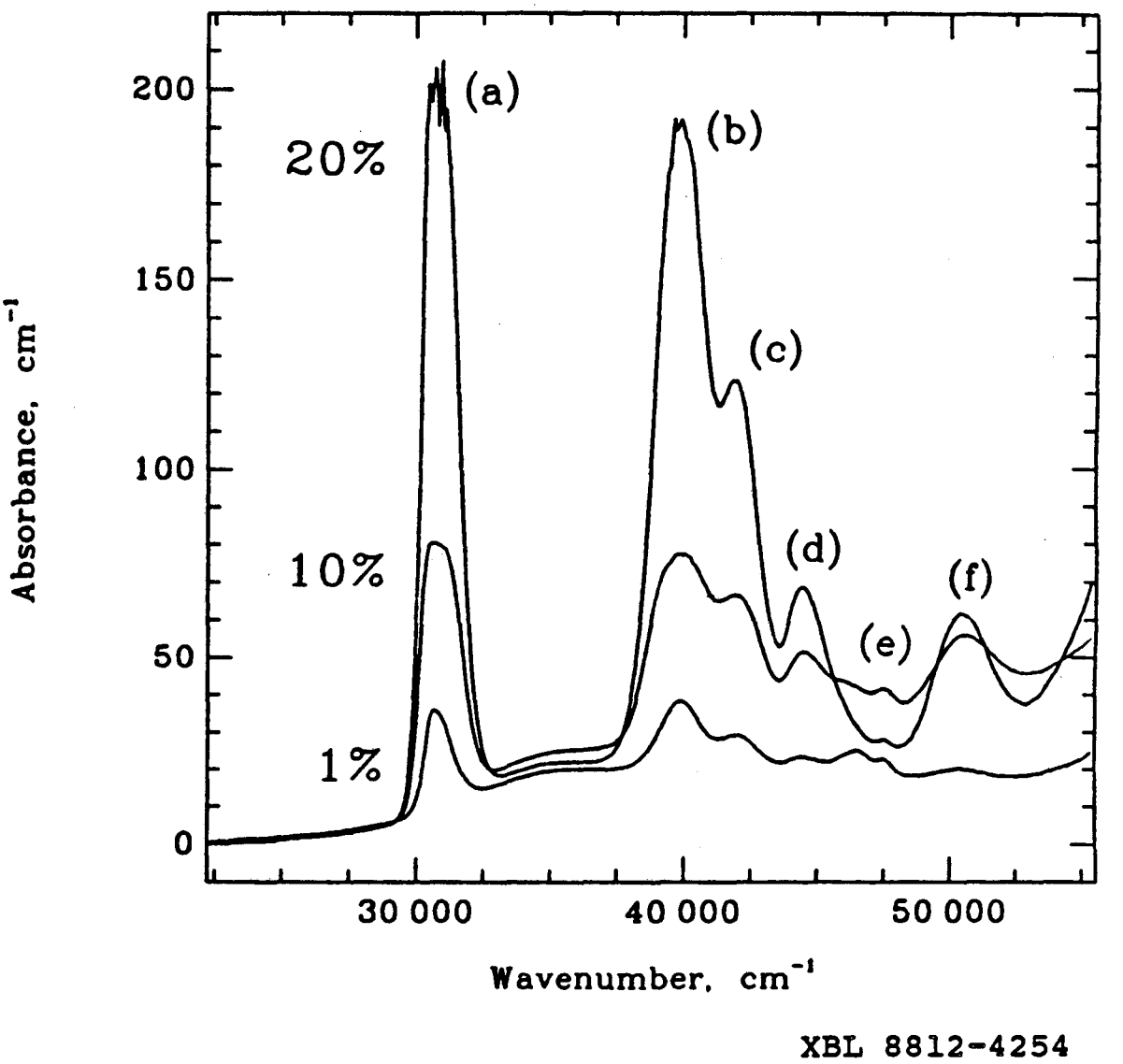

XBL 8812-4254

Figure 2

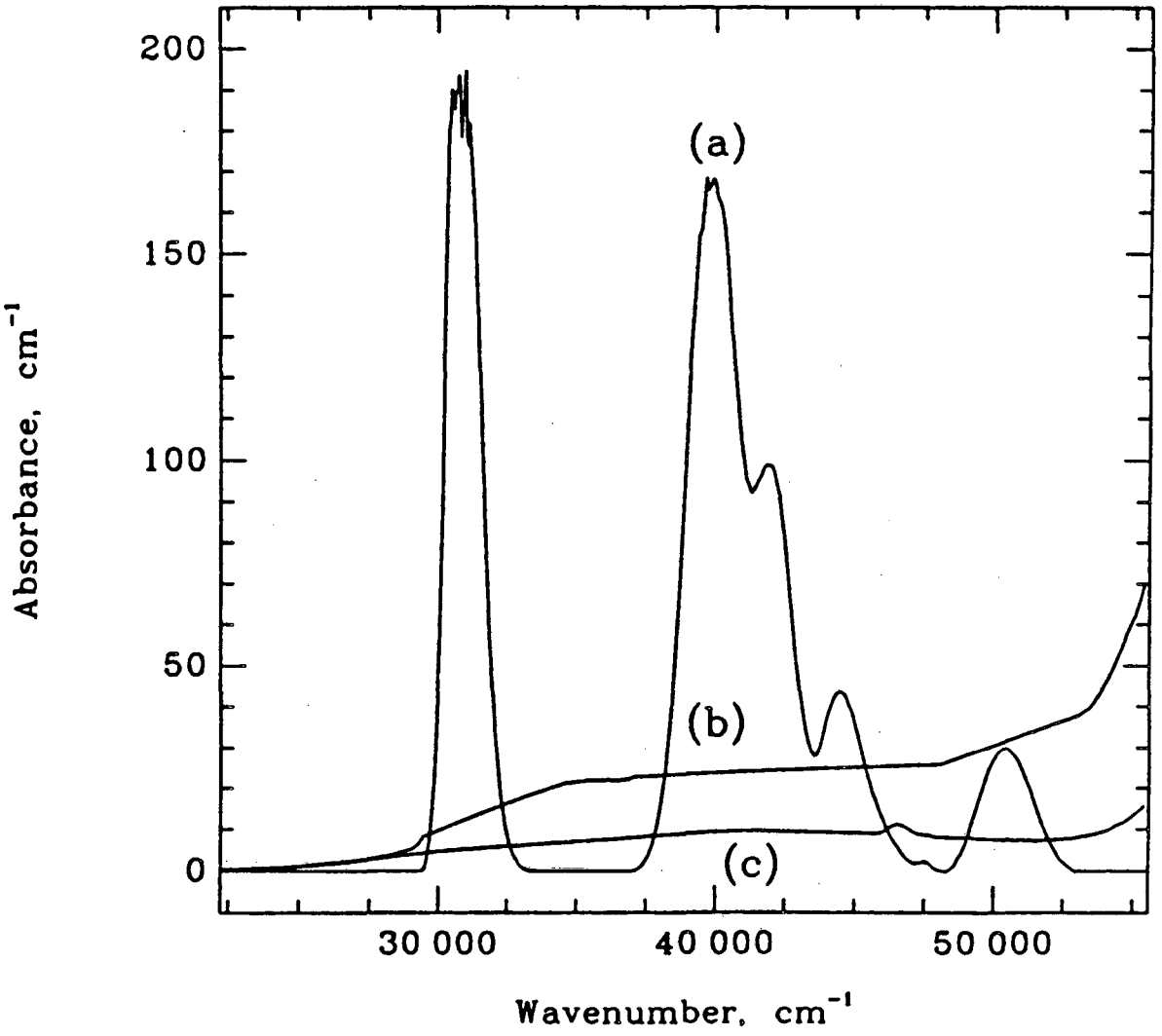

XBL 8812-4259

Figure 3

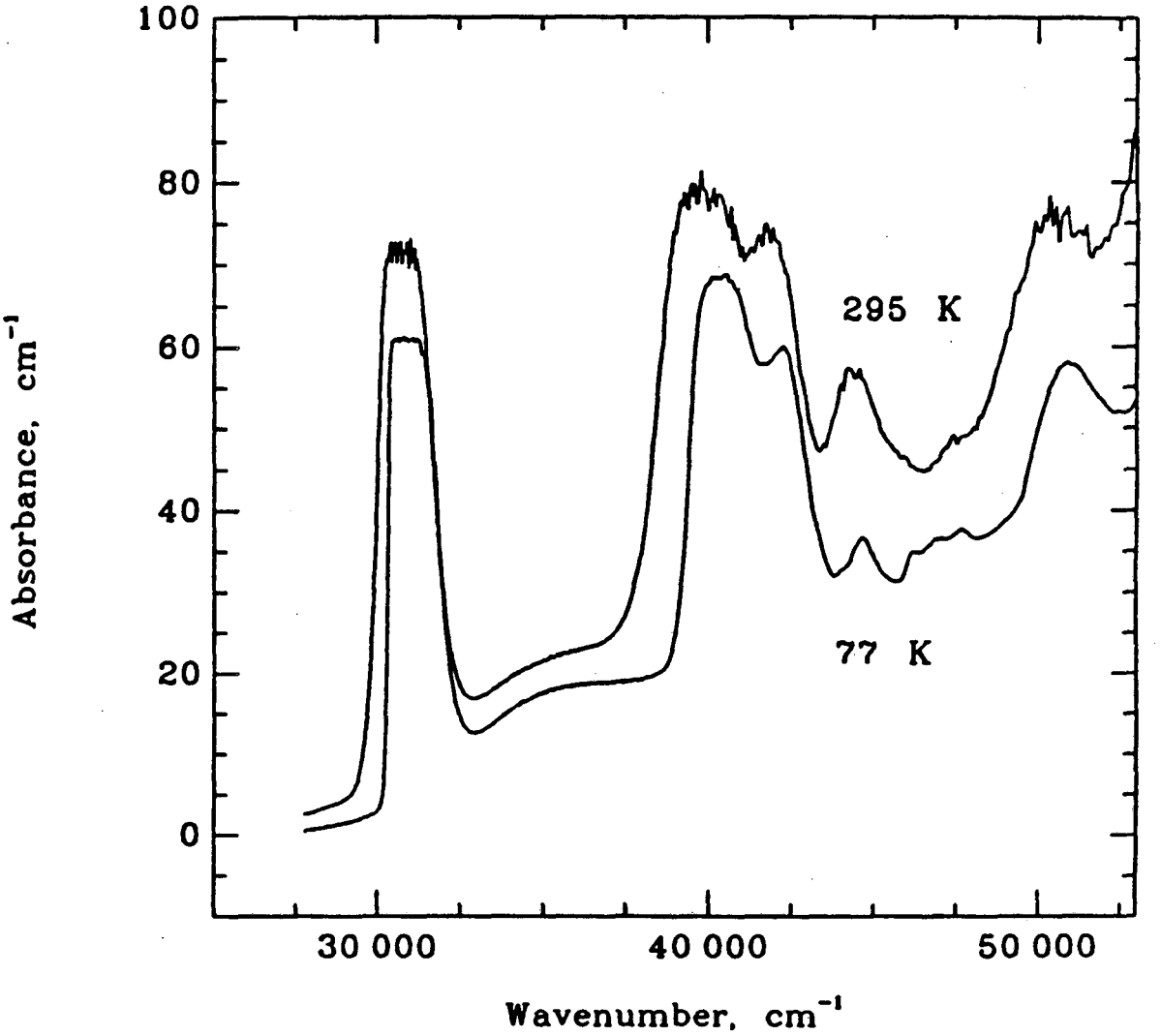

XBL 8812-4258

Figure 4

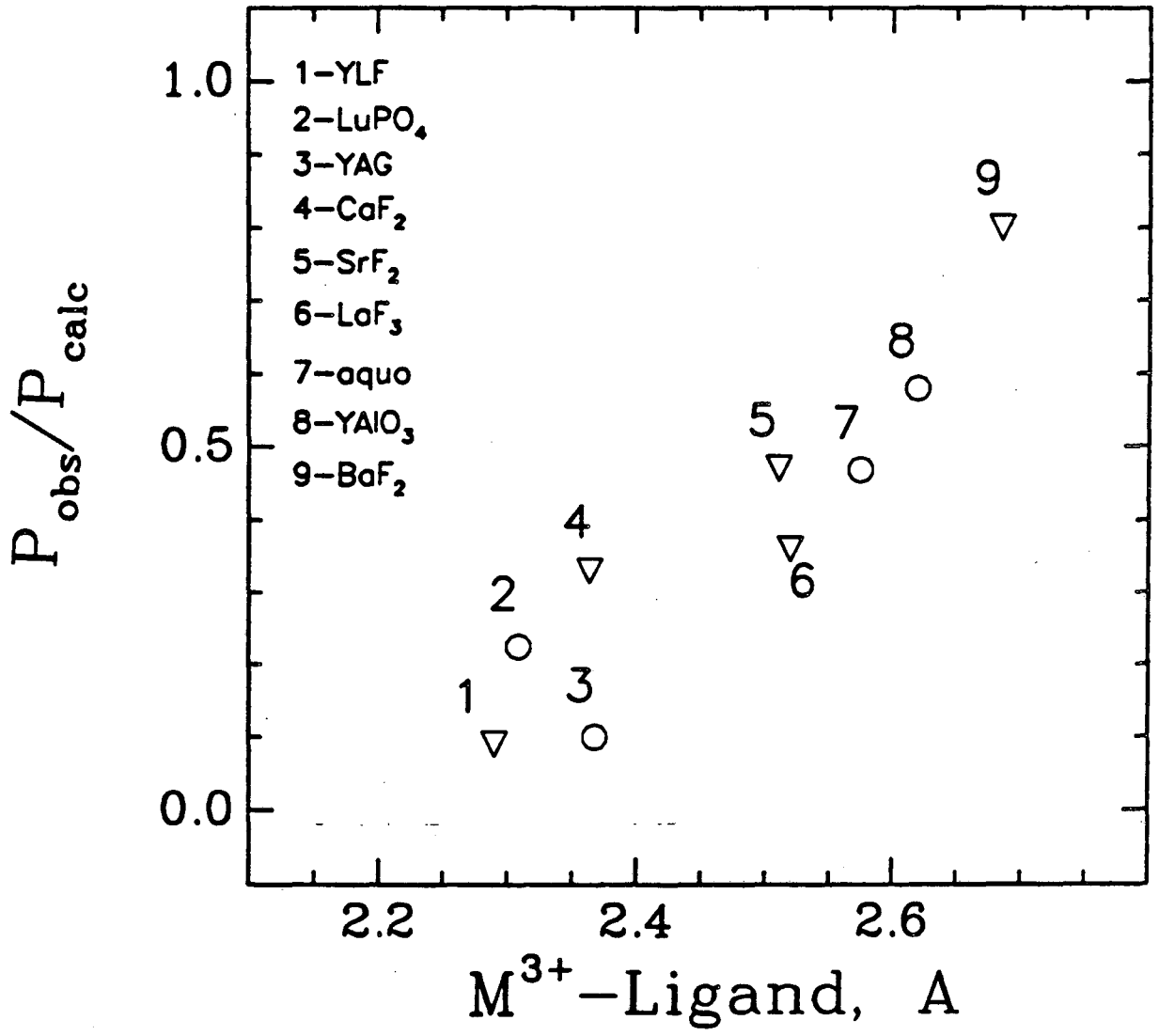

XBL 8812-4257

Figure 5

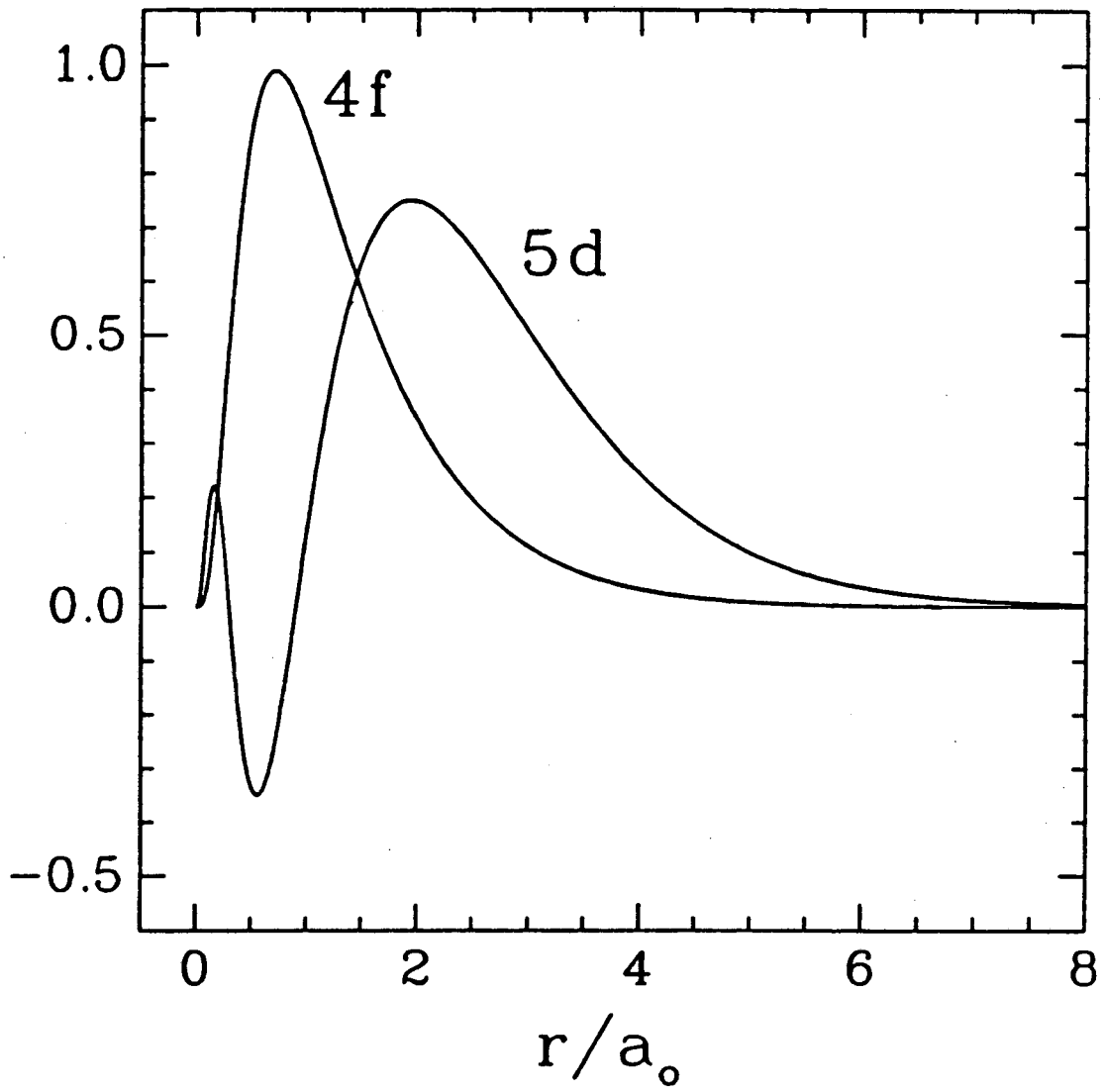

XBL 8812-4256

Figure 6

LAWRENCE BERKELEY LABORATORY
TECHNICAL INFORMATION DEPARTMENT
1 CYCLOTRON ROAD
BERKELEY, CALIFORNIA 94720